Influence of the Bénard Rolls on the Traveling Impulse in the Belousov−Zhabotinsky Reaction

B. Legawiec and A. L. Kawczyński*

Institute of Physical Chemistry, Polish Academy of Science, Kasprzaka 44/52, 01-224 Warsaw, Poland

Received: June 20, 1997; In Final Form: August 4, 1997[⊗]

A model of a chemical system in which the traveling impulse is affected by externally imposed natural convection in the form of the Bénard rolls is considered. The traveling impulse is described by the two-variable model of the B−Z reaction in an excitable regime. Numerical solutions to corresponding reaction−diffusion−convection equations show that the natural convection can generate a train of pulses of excitation, which are created from the single traveling impulse. The subsequently generated pulses spread alternately in the same and in the opposite directions as the initial traveling impulse, and they exhibit some type of translational delayed symmetry.

I. Introduction

Chemical waves create density gradients caused by concentrations gradients. Moreover, the temperature gradient can be created due to reaction heat and it can affect the density gradient. If the density gradient has a nonvanishing component perpendicular to the gravitational field, then natural convection appears always in liquid systems.[1] Natural convection does not appear only if the chemical wave has the form of a traveling front that spreads vertically and the density increases downward. However, also in this case one cannot exclude natural convection because of the so-called double-diffusion phenomenon.[2,3] All other chemical waves (single traveling impulses, trains of traveling impulses, spiral waves) appearing in liquid systems generate natural convection.

Although traveling waves almost always generate natural convection, experimental measurements of the convection patterns are rare. The convection pattern caused by the trains of the traveling impulses in the B−Z reaction has been measured directly.[4] The oscillations in the velocity of natural convection have been discovered. Most of experimental works have been concerned with studies of an influence of natural convection on traveling fronts.[5−15] The experiments were usually performed in thin tubes without thermostating of the systems. Several chemical reactions have been studied: iron(II)−nitric acid,[5,8] iodate−sulfite,[13,15] bromate−sulfite,[13,14] chlorate−sulfite,[10] iodate−arsenous acid, [7,12] chlorite−thiosulfate,[6] and chlorite−tiourea.[11] Natural convection causes the curvature of the fronts and changes substantially their velocity as compared with convectionless conditions. For example, the traveling front in the nitric acid−iron(II) reaction in a thin tube spreads downward with a velocity from 4 to 10 times larger than that upward.[5] In several cases the "finger" concentration patterns, due to the double-diffusion effect, were observed.[8−11,15]

Natural convection disturbs a traveling wave, and the disturbed wave affects the convection pattern. Therefore, to describe the chemical wave, which is disturbed by natural convection, it is necessary to use reaction−diffusion−convection equations instead of reaction−diffusion equations. The fundamental problem that appears here is the determination of a natural convection pattern. It is necessary to solve simultaneously the Navier−Stokes equation and balance equations for mass and internal energy. The last two equations must include corresponding convection terms, whereas the term with buoyancy force in the Navier−Stokes equation should contain the density distribution determined by the reagents concentrations and the temperature fields. It is assumed that an equation of state is known that allows the determination of the density distribution from known concentration and temperature distributions.

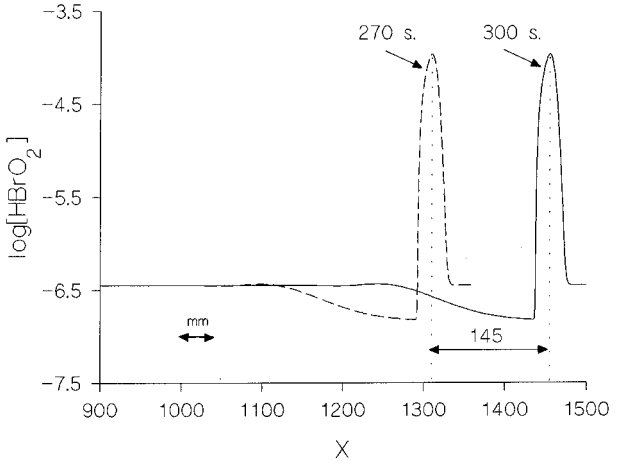

Figure 1. Distribution of the concentration of $HBrO_2$ in a one-dimensional system after 210 and 300 s. The *X* axis is given as the number of steps from the center of the system (one step equals 0.025 mm).

The influence of natural convection on chemical waves has been discussed mainly in a qualitative way.[3,5−15] Quantitative solutions have been obtained for very simple models only. The front traveling vertically in systems with various geometries has been replaced by the jump in density (the so-called eikonal relation), and linear stability theory was used to determine natural convection pattern from the Navier−Stokes equation.[16−21] For traveling fronts described by the Schlögel type kinetics that generate continuous changes in density, the linear stability analysis of the Navier−Stokes equation has been supported by numerical calculations.[22,23] Transitions between convection patterns dependent on the geometry of the system have been predicted.[23] The obtained results confirm experimental observations that natural convection induces the curvature of traveling fronts. The influence of natural convection appearing in the electro-thermodiffusion method on the Schlögel type traveling front has been studied numerically.[24] In this case, the influence

[⊗] Abstract published in *Advance ACS Abstracts,* September 15, 1997.

S1089-5639(97)02021-5 CCC: $14.00 © 1997 American Chemical Society

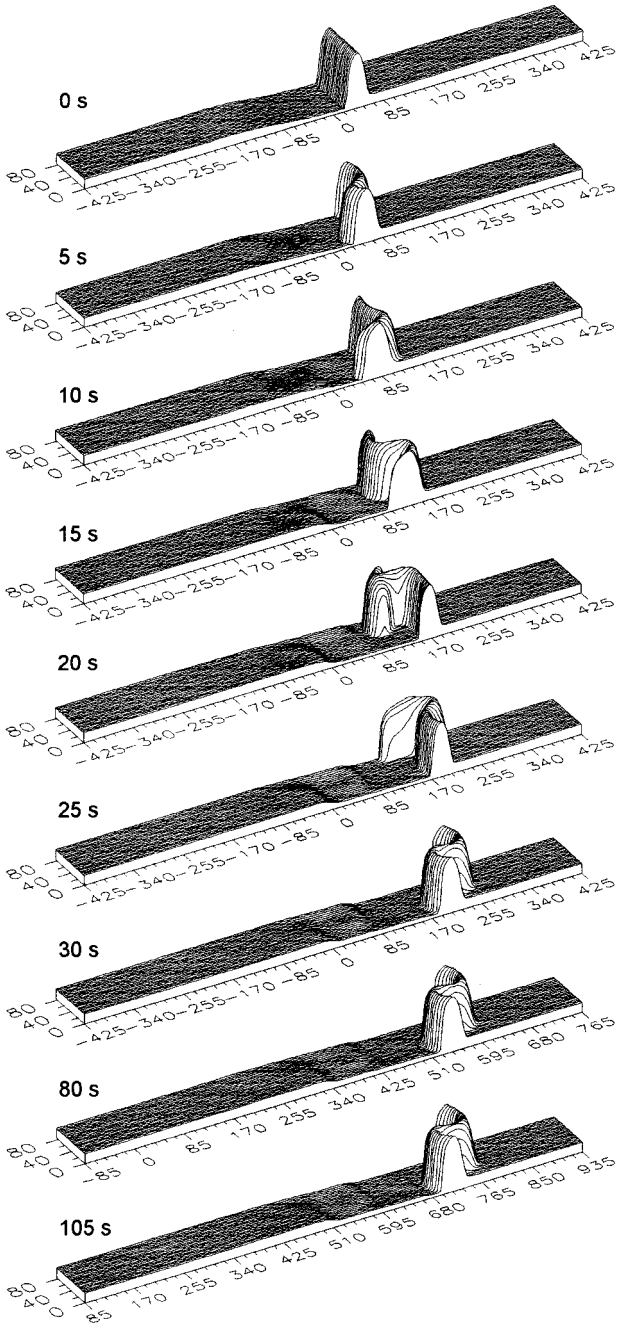

Figure 2. Two-dimensional snapshots showing the evolution of the concentration distribution of $HBrO_2$ for $r = 1$. Both axis are described as the numbers of their size steps. Five pairs of the rolls are shown.

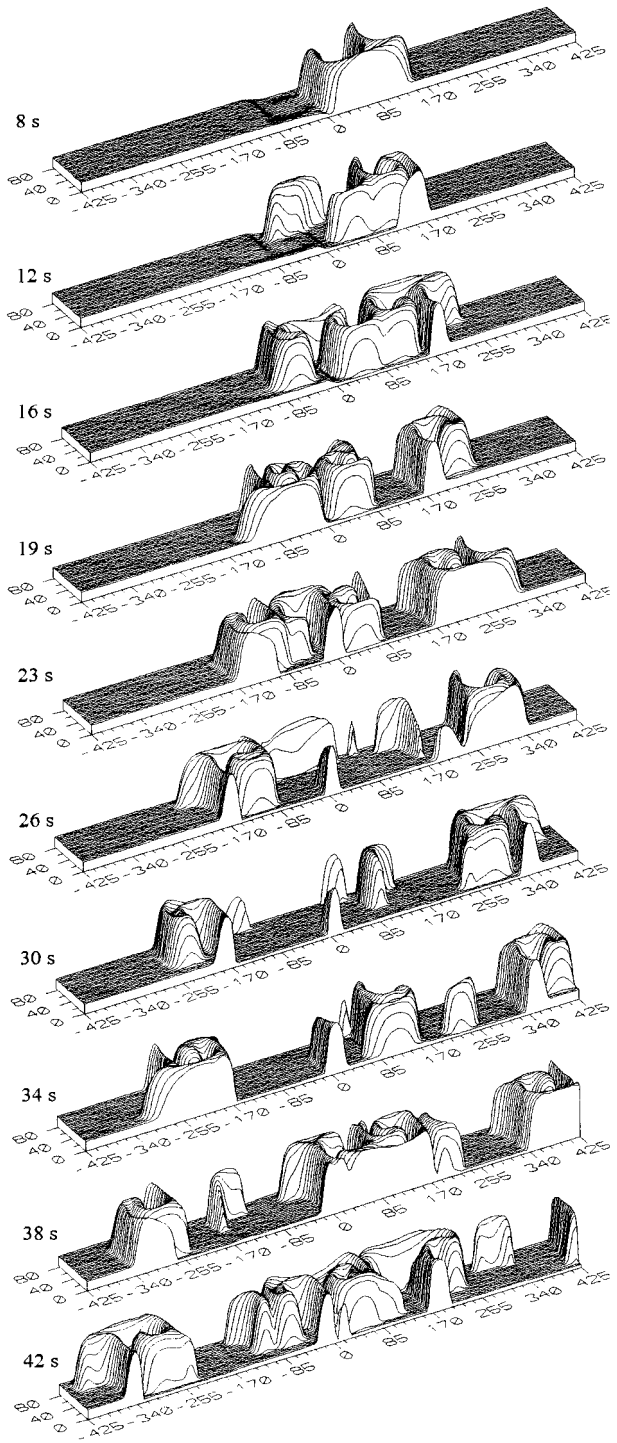

Figure 3. Same as in Figure 2 but for $r = 3$. Five pairs of the mid-rolls are shown only.

of the front on the convection pattern has been neglected. Similar simplification has been used in the study of the influence of the Bénard rolls on the same front.[25] In these cases natural convection changes substantially the shape of the front and increases its velocity. An influence of natural convention on the traveling impulse described by the two-variable Oregonator model has been studied by the linear stability analysis of the Navier−Stokes equation combined with numerical calculations.[26] The results obtained for various geometries of the system are in qualitative agreement with the experimental observations. Convection patterns caused by stationary distributions of concentrations having the form of one or more pulses have been studied numerically.[27] The results obtained are in agreement with the experimental observations of oscillations of velocity of convection in the B−Z system.[4] In all cases described above qualitative properties of the waves remain unchanged. The flat fronts become curved, and the shape of the impulses is changed. Qualitative changes such as divisions of the chemical waves do not appear.

In the present paper we study the influence of externally imposed fluid motion on traveling impulses. In our model a chosen convection pattern can change qualitative properties of the impulse as compared with convectionless conditions. A division of the traveling impulse can appear. The two-variable model of the Belousov−Zhabotinsky reaction in an excitable regime[28] is chosen to generate traveling impulses in spatially distributed systems. Moreover, we assume that a vertical temperature gradient generates the convection pattern (the Bénard rolls), which can be described in a two-dimensional geometry.[29] To simplify the problem, we neglect the affect of

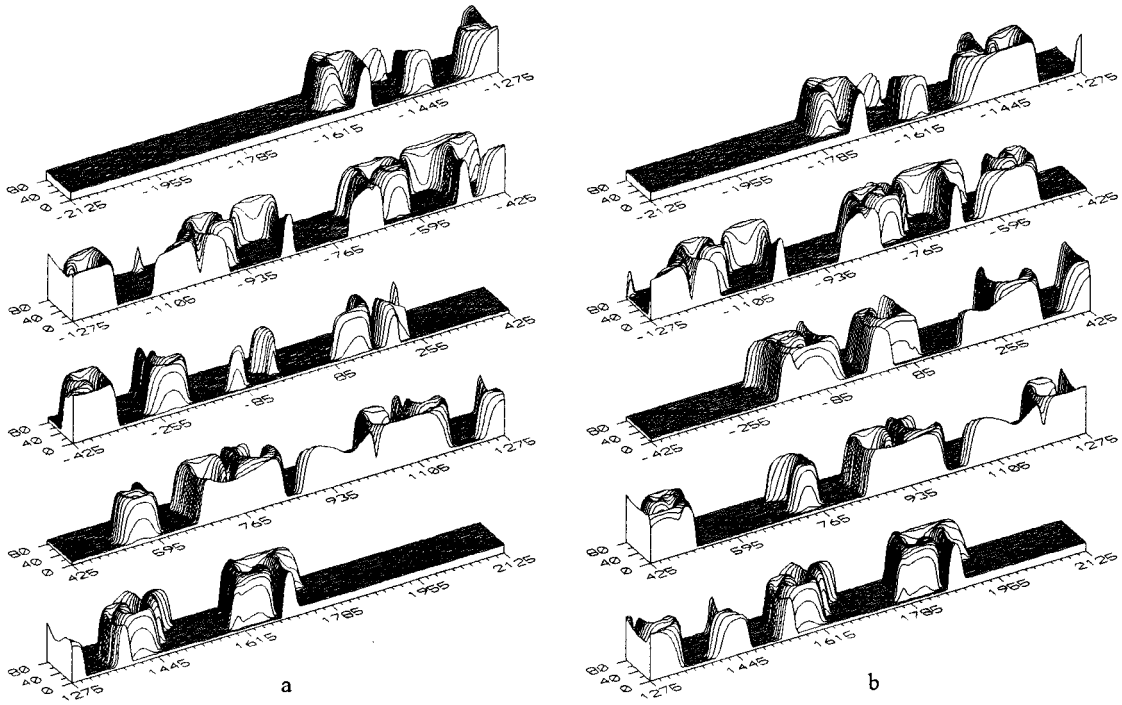

Figure 4. Snapshots of the concentration distribution of $HBrO_2$ for $r = 3$ at selected moments of the time showing the symmetry given by eq 7: (a) $t = 150$ s and (b) $t = 165$ s. Twenty-five pairs of the rolls are shown.

the density distribution generated by the impulse on the convection pattern. This simplification is reasonable if the density distribution is determined not only by the concentration distribution generated by the traveling wave but also by the temperature distribution that generates the Bénard rolls. The contribution to the density distribution coming from the traveling wave can be much smaller as compared with the temperature gradient. For the Bénard rolls the solution to the Navier−Stokes equation is known in explicit form, and we will use this solution in the convection term of the kinetic equation. In this way the influence of the traveling wave on a pattern of natural convection is neglected, but the influence of the convection on the concentration distribution is taken into account.

The paper is organized as follows. In section II a model describing the traveling impulse is presented. In section III the Bénard rolls are described, and in the next section the reaction−diffusion−convection model is formulated. In section V the obtained results are presented and discussed. In last section we present conclusions that follow from our results.

II. Model of Traveling Impulses

Dynamics of the B−Z reaction (bromate, bromomalonic acid, ferroine, and sulfuric acid) in some range of initial concentrations of the reactants can be described by two kinetic equations.[28,30−31] These equations are based on the Field−Körös−Noyes mechanism.[32] It is convenient to write them in the form in which concentrations are used as dimensionless variables whereas time is a dimensional variable:

$$\frac{dc_1}{dt} = \epsilon\left[c_1(1-c_1) - \left(2q\alpha_1\frac{c_2}{1-c_2} + \beta\right)\frac{c_1-\mu}{c_1+\mu}\right] = F_1(c_1,c_2) \tag{1a}$$

$$\frac{dc_2}{dt} = \gamma\left(c_1 - \alpha_1\frac{c_2}{1-c_2}\right) = F_2(c_1,c_2) \tag{1b}$$

where

$$[\mathrm{Fe(phen)_3^{3+}}] = Cc_2, \quad [\mathrm{HBrO_2}] = \frac{k_1A}{2k_4}c_1, \quad \epsilon = k_1Ah_0,$$

$$\alpha_1 = \frac{k_4K_8B}{(k_1Ah_0)^2}, \quad \beta = \frac{2k_4k_{13}B}{(k_1A)^2h_0}, \quad \gamma = \frac{(k_1A)^2h_0}{k_4C}, \quad \mu = \frac{2k_4k_7}{k_1k_5},$$

$$A = [\mathrm{NaBrO_3}], \quad B = [\mathrm{CHBr(COOH)_2}],$$

$$C = [\mathrm{Fe(phen)_3^{2+}}] + [\mathrm{Fe(phen)_3^{3+}}]$$

h_0 is the acidity function (unit M = [mol/L]), q is the stoichiometric factor, and k_i are the rate constants. In sequel we will use the values of the parameters, which are identical with those in[31]

$$k_1 = 100\ \mathrm{M^{-2}\,s^{-1}}, \quad k_4 = 1.7\times10^4\ \mathrm{M^{-2}\,s^{-1}},$$
$$k_5 = 10^7\ \mathrm{M^{-2}\,s^{-1}}, \quad k_7 = 15\ \mathrm{M^{-2}\,s^{-1}},$$
$$K_8 = 2\times10^{-5}\ \mathrm{M\,s^{-1}}, \quad k_{13} = 10^{-6}\ \mathrm{s^{-1}}, \quad q = 0.5$$

For these values of the parameters in a broad range of the reactant concentrations the nullcline for c_1 has an inverse N shape, whereas the nullcline for c_2 is an increasing function of c_1. These curves can intersect themselves in one point only, which corresponds to a stationary state. Equations 1, for some values of the reactants concentrations, describe simple, periodic in time oscillations of $[\mathrm{Fe(phen)_3^{3+}}]$, which agree well with the experiments performed in the batch reactor.[30,33] For the following reactants concentrations, $B = 0.775$ M, $A = 0.01$ M, $C = 6.5\times10^{-4}$ M, and $h_0 = 0.15$ M, system 1 is in the excitable regime and in this case one can expect an appearance of the traveling impulse.

The behavior of spatially distributed system is described by reaction−diffusion equations in the form

$$\frac{\partial c_i}{\partial t} - D_i\frac{\partial^2 c_i}{\partial X^2} = F_i(c_1,c_2) \qquad i = 1, 2 \tag{2}$$

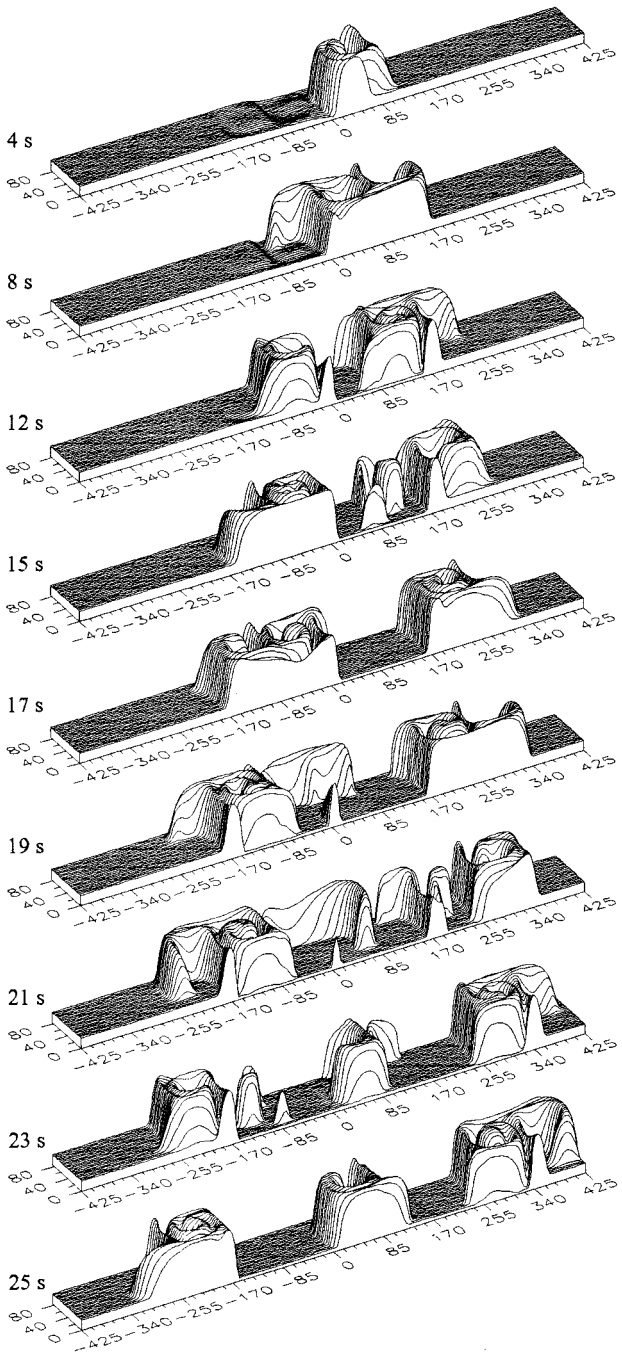

Figure 5. Same as in Figure 3 but for $r = 5$.

where $F_1(c_1,c_2)$ and $F_2(c_1,c_2)$ are equal to the right-hand sides of eqs 1a,b and D_1 and D_2 are diffusion coefficients of $[HBrO_2]$ and $[Fe(phen)_3^{3+}]$. The formation of the traveling impulse caused by a local disturbance of the concentration above the threshold value was confirmed by numerical solution of the reaction−diffusion equations, eqs 2. In our calculations we assumed: $D_1 = D_2 = 4 \times 10^{-5}$ cm^2/s. The numerical solutions were performed for a finite in space system with zero-flux boundary conditions. However, the size of the system was so large that gradients of the concentrations close to the boundaries were negligibly small and the part of the impulse between its "front" and "back" remained far from the boundaries and occupied a small interval in our system. The profile of the $HBrO_2$ concentration is shown in Figure 1. One can easily see the "front" and the "back" of the impulse. Just behind the back there is the region in which the concentration of $HBrO_2$ falls down below the stationary value to so-called refractory region. Next the concentration of $HBrO_2$ grows and approaches its stationary value. The repeated disturbance will generate the next traveling impulse.

For the values of the given parameters the traveling impulse has the velocity equal to 0.12 mm/s and its "width", which is the distance between the front and the back is equal to 1.02 mm.

III. Bénard Rolls

In an infinite horizontal fluid layer heated from below, natural convection appears if a critical value of the Rayleigh number is exceeded. The Rayleigh number is defined by

$$Ra = \frac{g\alpha\Delta T d^3}{\kappa\nu} \tag{3}$$

where g is the acceleration due gravity, α the coefficient of volume expansion, ΔT the temperature difference, d the depth of the layer, κ the coefficient of thermometric conductivity, and ν the coefficient of kinematic viscosity.

The onset of instability is manifested as the appearance of a nonvanishing disturbance of convection velocity with a particular wavenumber. For rigid boundaries the critical value of the Rayleigh number is $Ra_c = 1707.762$. The horizontal period of the convection pattern is given by $L = 2\pi d/a_c$, where the critical value of the dimensionless wavenumber $a_c = 3.117$.[29] Various convection patterns (hexagons, rolls) are possible. Hexagonal patterns need three-dimensional geometry and therefore, are much more time and memory consuming in numerical calculations that must be used to solve a reaction−diffusion−convection equation. In the case of rolls we have a two-dimensional geometry. Only one of the horizontal coordinates, say X, is sufficient. For simplicity, in this paper the convection pattern in the form of the rolls is considered.

In the dimensionless coordinates $z = Z/d$ and $x = X/d$, the vertical v_z and horizontal v_x components of the convection velocity for the rolls are defined by:[29]

$$v_z = A_1 \cos(a_c x) W(z) \tag{4a}$$

$$v_x = -\frac{A_1}{a_c} \sin(a_c x) \frac{dW(z)}{dz} \tag{4b}$$

where

$$W(z) = \cos(q_0 z) - a_1 \cosh(q_1 z) \cos(q_2 z) + a_2 \sinh(q_1 z) \sin(q_2 z)$$

and

$$a_1 = 0.061\,510\,563\,9, \quad a_2 = 0.103\,886\,7,$$
$$q_0 = 3.973\,639, \quad q_1 = 5.194\,989\,7, \quad q_2 = 2.126\,287\,6$$

and A_1 is the amplitude of the convection velocity[29]

$$A_1 = \sqrt{80.23\left(\frac{\kappa}{d}\right)^2\left(\frac{Ra}{Ra_c} - 1\right)}$$

In eqs 4 the variable z changes in the limits $-1/2 \le z \le 1/2$.

IV. Reaction−Diffusion−Convection Model

Let us assume now that the traveling impulse is generated in an infinite horizontal layer with the B−Z reaction mixture in which natural convection has the form of the Bénard rolls. Local changes of the dimensionless concentrations of $[HBrO_2]$ and

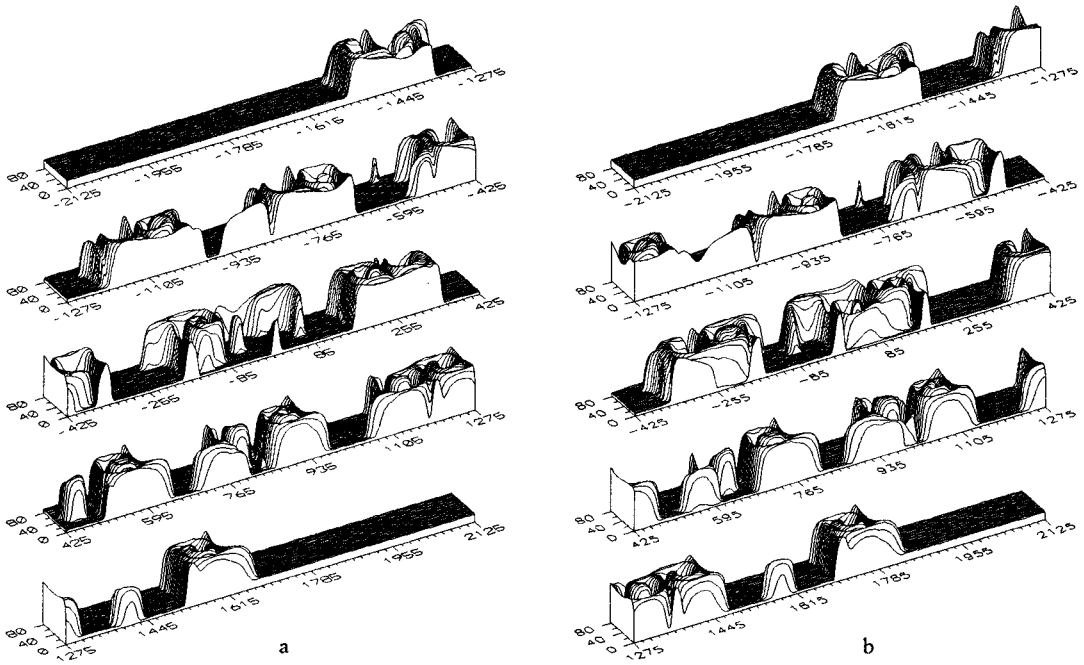

Figure 6. Same as in Figure 4 but $r = 5$ and at $t = 107$ s (a) and $t = 118$ s (b).

$[Fe(phen)_3^{3+}]$ are described by the reaction−diffusion−convection equations

$$\frac{\partial c_i}{\partial t} - D_i\left(\frac{\partial^2 c_i}{\partial X^2} + \frac{\partial^2 c_i}{\partial Z^2}\right) + v_x \frac{\partial c_i}{\partial X} + v_z \frac{\partial c_i}{\partial Z} = F_i(c_1,c_2) \quad i = 1, 2 \tag{5}$$

where v_x and v_z are horizontal and vertical components of the convection velocity in the Bénard rolls given by eqs 4a,b. For convenience, the time and the space coordinates have their usual dimensions. We want to stress that we neglect the influence of the density gradient generated by the traveling impulse on the convection pattern. Otherwise we should solve simultaneously eqs 5 and the Navier−Stokes equation, with the density distribution determined by the traveling impulse.

Since our system is infinite in the direction X, we assume the initial distributions of c_1 and c_2 in the form of the traveling impulse that is the asymptotic solution of eqs 2 (see Figure 1). At initial time the concentrations distributions are independent of the vertical coordinate Z. For the vertical coordinate Z we assume the zero-flux boundary conditions:

$$\left.\frac{\partial c_i}{\partial Z}\right|_0 = \left.\frac{\partial c_i}{\partial Z}\right|_d = 0 \tag{6}$$

For given values of the parameters in eqs 2, there are two free parameters, which to some extent, can be controlled in experiments. One of them is the ratio of "width" of the impulse to the period of the Bénard rolls. In the sequel we will assume that the "width" of the impulse is about half of the single Bénard roll. For the impulse that covers one or more rolls, one can expect the effects similar to those observed in the model with the traveling front.[25] On the other hand, if the impulse is too narrow, then the numerical calculations need much more powerful computer than we have available. The other free parameter (r) is the ratio of a maximal convection velocity to the traveling impulse velocity in the convectionless system. In our calculations the velocity of the traveling impulse was constant, and we changed A_1 so that the ratio r was equal to 1, 3, 5, and 7.

V. Results and Discussion

Equations 5 were solved numerically on two-dimensional lattice covering an integral number of pairs of the Bénard rolls. The initial value problem with respect to the X coordinate was replaced by the boundary value problem with the zero-flux boundary conditions. All calculations were started from five pairs of the rolls. We numerate the rolls from the mid-pair by the first right (left) roll, the second right (left) roll, and so on. If the concentrations of c_1 and c_2 at the right or left boundary roll become different by assumed value from the stationary state, then we enlarge the system by a pair of the rolls with the concentrations c_1 and c_2 equal to their stationary values. Each pair of the rolls was divided into 170 equal distance steps along the X coordinate and 85 along the Z direction. Let us mention that the space step in the X direction is a little larger than the step in Z direction and their ratio is equal to 1.007 86. We have used the Crank−Nicolson scheme in calculations of the spatial distributions of c_1 and c_2, and we have applied the four-stage Runge−Kutta method in order to calculate the kinetic terms.

The results of numerical solution of the problem for $r = 1$ are shown in Figure 2. In this figure as well as in the next figures, X and Z coordinates are given as the number of grid points from the center of the system. The initial impulse is bending along X and Z according to the convection pattern and spreads to the right with "jumping" velocity. After a transient regime (about 30 s), the distributions of c_1 and c_2 approach their asymptotic forms, which have the following symmetry property:

$$c_i(X,Z,t) = c_i(X+L,Z,t+T) \tag{7}$$

This property means that the concentration distribution that is shifted back along the X coordinate by one pair of the rolls (the period of convection pattern L) is the same as the nonshifted distribution was at the time period T earlier. For $r = 1$ we observed time−space evolution of the single impulse of excitation.

The behavior of the systems changes qualitatively for $r = 3$. The beginning of evolution of the initial traveling impulse is shown in Figure 3. The initial impulse, which at $t = 0$ s is in

the first right roll, is twisted and stretched. It would be misleading to call it "the impulse", and therefore, we will use the term "a pulse of excitation" to describe excited regions. As shown in Figure 3, the pulse of excitation envelops to the second right roll (see $t = 8$ s). Later on the pulse spreads also to the first left roll, and then its division into two pulses occurs (see $t = 12$ s). These two pulses, still twisting and stretching, join together and again form one pulse that extends over four rolls (see $t = 16$ s). Next this large pulse decomposes again into two pulses (see $t = 19$ s). The right pulse occupies the third right roll, and the left one extends over three rolls. These pulses undergo a complicated evolution. The right pulse spreads to the fourth right roll (see $t = 23$ s), and next it decomposes leaving excited pieces behind (see $t = 26$ s). Simultaneously the left pulse spreads to the opposite direction and also decomposes leaving two excited pieces of it behind (see $t = 26$ s). The excited pieces left by the both pulses join together (see $t = 30$ s and $t = 34$ s), and next they form a new large pulse of excitation in the first and the second right rolls (see $t = 38$ s). Whereas the right and the left pulses continue spreading in opposite directions (see $t = 42$ s), the complicated evolution in the mid-rolls produces the next pair of pulses; one of them follows the right pulse, and the other one spreads behind the left pulse. The process of joining of pieces of excitation left behind by pulses spreading to right and to left and the creation of the large pulse of excitation in the mid-rolls repeats itself. In this way the mid-rolls become a "source" of the train of pulses spreading alternately in opposite directions. This part of evolution is not shown here. In Figure 4 the distributions of c_1 at $t = 150$ and 165 s are shown, respectively. It is easy to see that these distributions exhibit the same type of symmetry as given by eq 7, if regions are limited to those outside of the initial five pairs of rolls ($-425 < x < 425$). We have not found any periodicity in the concentrations distributions in the mid-rolls. Each new pair of pulses that leave the region of the initial five rolls is created from slightly different distributions of c_1 and c_2.

The little simpler evolution of the initial traveling impulse is observed for $r = 5$. As it is shown in Figure 5 the pulse of excitation spreads into the second right roll (see $t = 4$s) and later on also to the first left roll (see $t = 8$s) and next decomposes into two pulses (see $t = 12$ s). These two pulses never join together, but one of them spreads to right and the other one to left (see $t = 15$ s). The left pulse leaves the long tail of excitation behind it (see $t = 19$ s), which joins with the tail left behind the right pulse (see $t = 21$ s). In this way in the first right roll the new pulse of excitation is formed (see $t = 23$ s and $t = 25$ s), which after twisting and stretching decomposes to the new pair of the pulses. The process of joining of tails of excitations left behind the pulses repeats itself, and similarly as in the previous case the mid-rolls become the source of a train of pulses spreading alternately to the right and left. In Figure 6 the distributions of c_1 at $t = 107$ and 118 s are shown. As it is seen in this case the symmetry given by eq 7 is fulfilled only by the most outside pulses. The pulses that follow behind them satisfy this symmetry but with a slightly smaller time period T.

Further increment of r to 7 does not cause significant changes in the character of evolution as compared with the previous case. The initial period of the evolution is shown in Figure 7. The twisting and stretching of pulse is followed by its division into two pulses spreading to the right and to the left. In the mid-rolls the new pulse is formed from the tails of excitations left by the pulses. This pulse generates the new pair of pulses and so on. The region of the mid-rolls becomes the source of pulses

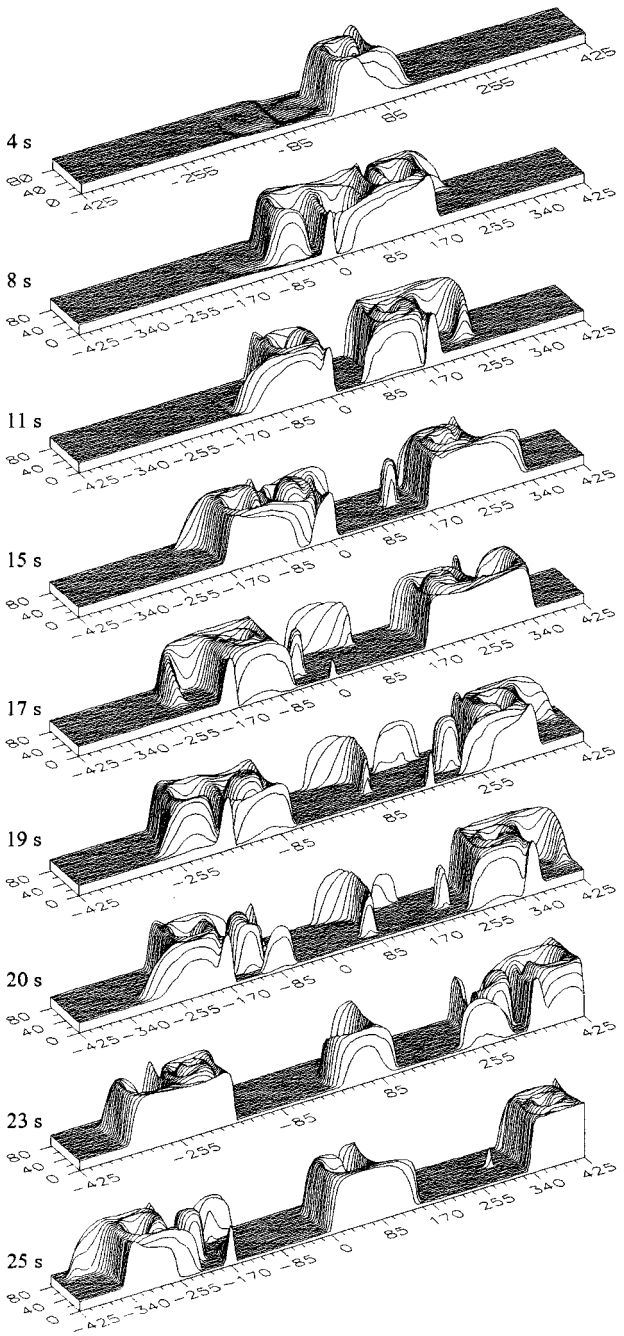

Figure 7. Same as in Figures 3 and 5 but for $r = 7$.

spreading alternately to the right and to the left. In Figure 8 the distributions of c_1 at $t = 101$ and 120 s are shown. The symmetry given by eq 7 is limited to the most outside pulses only. The pulses that follow them also have the same type of symmetry but with a smaller value of the period T.

The apparent velocity with which the pulses are spreading in the horizontal direction can be defined by the ratio of L and the corresponding time period T. Values of this apparent velocity are 0.12, 0.17, 0.28, 0.38, and 0.45 (mm/s) for $r = 0$, 1, 3, 5, and 7, respectively.

VI. Conclusions

The results presented above show that the convection transport can change in a qualitative way the evolution of concentrations distributions as compared with convectionless conditions. In the particular case considered in the present paper natural convection can induce the division of pulses of excita-

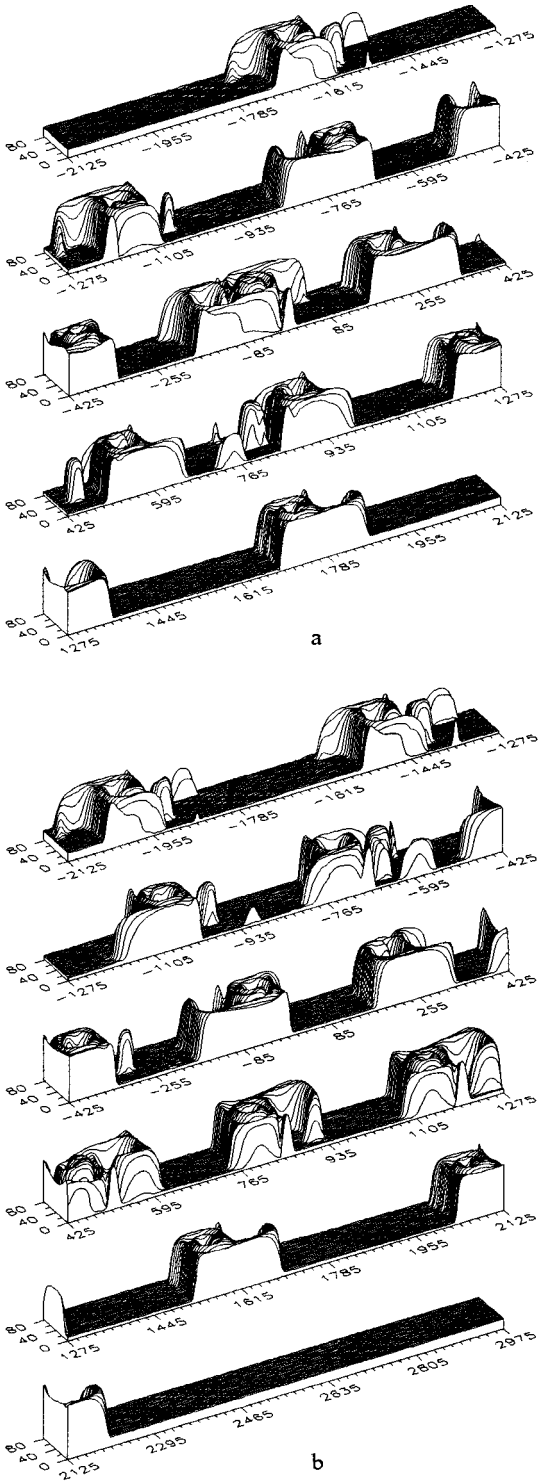

Figure 8. Same as in Figure 4 but for $r = 7$ and at (a) $t = 101$ s, 25 pairs of the rolls and (b) $t = 120$ s, 30 pairs of the rolls.

tions which in consequence causes the creation of train of pulses spreading alternately in opposite directions. The division of the initial traveling impulse occurs if the ratio of the maximal velocity of natural convection to the velocity of the traveling impulse is sufficiently large. There is some critical value of this ratio that must be exceeded in order to induce the division of pulses of excitation. In our system the critical value is between 1 and 3. Below the critical value only the initial traveling impulse is deformed (see Figure 2).

Our system is composed from the realistic model of the chemical wave and the convection pattern that can be observed in real systems. We want to stress that such composition can be performed experimentally. The other story is that the experiments can be difficult to perform. However, the effect of division of pulses of excitation described in this paper can appear spontaneously in thin layers of reaction mixtures with free surfaces in which a vertical temperature gradient can be generated by the evaporation of the mixture. In this case natural convection can appear due to the Maragoni effect caused by the variation of surface tension with temperature.[34]

References and Notes

(1) Kawczyński, A. L.; Baranowski, B. *Rocz. Chem.* **1973**, *47*, 1533.
(2) Turner, J. S. *Buoyancy Effects in Fluids;* Cambridge University Press: Cambridge, 1973.
(3) Pojman, J. A.; Epstein, I. R. *J. Phys. Chem.* **1990**, *94*, 4966.
(4) Miike, H.; Müller, S. C.; Hess, B. *Chem. Phys. Lett.* **1988**, *144*, 515.
(5) Bazsa, G.; Epstein, I. R. *J. Phys. Chem.* **1985**, *89*, 3050.
(6) Nagypal, J.; Bazsa, G.; Epstein, I. R. *J. Am . Chem. Soc.* **1986**, *108*, 3635.
(7) Pojman, J. A.; Epstein, I. R.; McManus, T. J.; Showalter, K. *J. Phys. Chem.* **1991**, *95*, 1299.
(8) Pojman, J. A.; Nagy, I. P.; Epstein, I. R. *J. Phys. Chem.* **1991**, *95*, 1306.
(9) Pojman, J. A.; Craven, R.; Khan, A.; West, W. *J. Phys. Chem.* **1992**, *96*, 7466.
(10) Nagy, I. P.; Pojman, J. A. *J. Phys. Chem.* **1993**, *97*, 3443.
(11) Chinake, C. D.; Simoyi, R. H. *J. Phys. Chem.* **1994**, *98*, 4012.
(12) Masere, J.; Vasquez, D. A.; Edwards, B. F.; Wilder, J. W.; Showalter, K. *J. Phys. Chem.* **1994**, *98*, 6505.
(13) Keresztessy, A.; Nagy, I. P.; Pojman, J. A. *J. Phys. Chem.* **1995**, *99*, 5379
(14) Nagy, I. P.; Keresztessy, A.; Pojman, J. A. *J. Phys. Chem.* **1995**, *99*, 5385.
(15) Pojman, J. A.; Komlósi, A.; Nagy, I. P. *J. Phys. Chem.* **1996**, *100*, 16209.
(16) Edwards, B. F.; Wilder, J. W.; Showalter, K. *Phys. Rev. A* **1991**, *43*, 749.
(17) Vasquez, D. A.; Edwards, B. F.; Wilder, J. W. *Phys. Rev. A* **1991**, *43*, 6694.
(18) Wilder, J. W.; Edwards, B. F.; Vasquez, D. A. *Phys. Rev. A* **1992**, *45*, 2320.
(19) Huang, J.; Vasquez, D. A.; Edwards, B. F.; Kolodner, P. *Phys. Rev. E* **1993**, *48*, 4378.
(20) Vasquez, D. A.; Wilder, J. W.; Edwards, B. F. *J. Chem. Phys.* **1993**, *98*, 2138.
(21) Huang, J.; Edwards, B. F. *Phys. Rev. E* **1996**, *54*, 2620.
(22) Vasquez, D. A.; Littley, J. M.; Wilder, J. W.; Edwards, B. F. *Phys. Rev. E* **1994**, *50*, 280.
(23) Wu, Y.; Vasquez, D. A.; Edwards, B. F.; Wilder, J. W. *Phys. Rev. E* **1995**, *52*, 6175.
(24) Otowska, M .; Kawczyński, A. L. *Pol. J. Chem.* **1992**, *66*, 697.
(25) Kawczyński, A. L.; Otowska, M. *Z. Phys. Chem.* **1994**, *186*, 171.
(26) Wu, Y.; Vasquez, D. A.; Edwards, B. F.; Wilder, J. W. *Phys. Rev. E* **1995**, *51*, 1119.
(27) Plesser, T.; Wilke, H.; Winters, K. H. *Chem. Phys. Lett.* **1992**, *200*, 158.
(28) Aliev, R. R.; Rovinsky, A. B. *J. Phys. Chem.* **1992**, *96*, 732.
(29) Chandrasekhar, S. *Hydrodynamic and Hydromagnetic Stability*; Clarendon Press: Oxford, 1961.
(30) Rovinsky, A. B.; Zhabotinsky, A. M. *J. Phys. Chem.* **1984**, *88*, 6081.
(31) Rovinsky, A. B. *J. Phys. Chem.* **1986**, *90*, 217.
(32) FIeld, R. J.; Körös, E.; Noyes, R. M. *J. Am. Chem. Soc.* **1971**, *94*, 8649.
(33) Zhabotinsky, A. M.; Buchholtz, F.; Kiytkin, A. B.; Epstein, I. R. *J. Phys. Chem.* **1993**, *97*, 7578.
(34) Koschmieder E. I. In *Advances in Chemical Physics; v. XXVI;* Prigogine I.; Rice S. A., Eds.; Wiley: New York, 1974; Vol. XXVI, p 177.